

## NUMERICAL MODEL OF LARGE-SCALE LEVITATION MELTING PROCESS

The levitation melting has a potentially wide range of applications, especially in the processing of reactive metals whose contact with the crucible material causes their contamination and damage to the crucible itself. Despite its advantages, levitation melting, already proposed in the 1920s, has not yet found significant use in industrial conditions. This is due to the nature of the electromagnetic field used in previously developed devices. The disappearance of this field in the system axis causes overcoming, in the case of larger charges, surface tension forces and metal leakage from the device. The article contains a comparative analysis of a conventional solution and a newly developed levitation melting device, whose completely different design eliminates the previous weight limit of the charge.

*Keywords:* levitation melting, reactive metals, numerical modelling

### 1. Introduction

Metal levitation melting seems to be a very interesting solution when the need of processing of highly reactive metals appears. The metals in the group which primarily includes titanium alloys in the molten state react with the vast majority of materials used for crucibles. This results not only in the destruction of the crucible itself, but mainly in the contamination of the processed metal.

So far, the melting in cold crucible devices [1] is a commonly used solution. With their application the liquid metal gets in contact with the water-cooled copper bottom of the crucible and a layer of solidified metal called a skull forms at the bottom of the charge. It protects the liquid reactive metal from the direct contact with the crucible material thus avoiding both the risk of contamination of the processed metal and damage of the crucible.

This solution of so-called semi-levitation melting, despite all its ingenuity, however, features a few closely related very important defects. The first disadvantage is a very low electrical efficiency of the device since the electromagnetic field generates most of Joule heat not as a useful heat for the charge, but as a loss in the structural parts of the cold crucible. The major losses are mainly generated in the bottom of the crucible which supports the charge and forms the skull. Moreover, the need for continuous cooling of this crucible component, in order to maintain the separating layer of the skull, means a continuous and unavoidable escape of heat from the system. This feature of the cold crucible device signifies that it also has very low thermal efficiency. As a result, the solutions with a cold crucible currently applied in

the melting process of reactive metals, despite some attempts on their modification [2-4], are characterized by dreadful weak overall efficiency which does not exceed several percent.

Full levitation melting equipment has much higher efficiency than the semi-levitation one. It is because in case of the former there is a total lack of contact between the metal and crucible as well as no need for placing the passive elements of a cold crucible, where power losses are generated, in the electromagnetic field. Therefore full levitation melting equipment should find its wide use in the processing of reactive metals. However, with all the advantages and despite numerous modifications, the levitation melting invented back in the 1920s [5], has not yet found its widespread application in industrial conditions. This is due to the nature of the electromagnetic field used in hitherto developed devices. In the case of conventional solutions, the molten charge is positioned in the axis of the device. In this area we are dealing with inevitable disappearance of the field of electromagnetic forces supporting the liquid metal. In the case of so far used small charges, the surface tension forces prevent metal leakage in this area. Unfortunately, in the case of larger than a few grams charges, the hydrostatic pressure overcomes the surface tension forces and metal leakage from the device occurs.

Only recently have the first effective attempts appeared at breaking the many years of stagnation in the development of these devices. The attempts went in the direction of increasing the mass of molten charges by revolutionizing the concept of levitation melting as such.

In [6] the authors proposed a complete change of the electromagnetic field orientation from vertical to horizontal which

\* SILESIAAN UNIVERSITY OF TECHNOLOGY, FACULTY OF MATERIALS ENGINEERING AND METALLURGY, KATOWICE, POLAND

# Corresponding author: Bogdan.Panic@polsl.pl

was aimed at eliminating the above-mentioned problem of the lack of charge support in the area of vertical axis of the system. As a result, it was possible to obtain the experimentally confirmed opportunity of melting the charges up to 33 g as well as a potential chance of melting those reaching 500 g. Although, the proposed solution breaks the stagnation in the development of levitation melting, it has its two important drawbacks. First and foremost, it requires the use of a complex dual-frequency power supply system which can limit the up-scaling of the solution. Besides, due to the use of a rotating magnetic field, some complications may occur with maintaining the stability of the charge during melting.

The solution discussed in the paper and referred to in the patent application PL427317 from 2018 is the second attempt recently made to change the basic concept of levitation melting. The issue of disappearance of the electromagnetic force field in the axis of the system was solved here by modifying the geometry of the inductor and moving the charge away from the area of the vanishing field. Thanks to the single-frequency power supply of the inductor and the quasi-static alternating electromagnetic field, the proposed solution has a considerable potential for melting charges of a large mass.

Numerical modeling is becoming more and more popular in the field of both metallurgical [7-14] and nonferrous metallurgical processes [15-21]. Also, the levitation melting analysis presented in the article was based on the numerical model. The article describes the model which aimed at determining the distribution of forces acting on the metal charge in the device as well as Joule heat generated in the charge. On the basis of this model the authors analyzed the reasons why the large charges could not be molten in classical levitation melting devices and confirmed by numerical simulation the potential capabilities of the newly developed device. The obtained simulation results proved that the proposed new solution of the levitation melting device effectively eliminates the basic problem which so far has hindered the effective application of this process for a scale greater than a laboratory scale.

## 2. The model of levitation melting

The numerical model of this process was a tool for conducting comparative analysis of two conceptual proposals of levitation melting system.

Due to the geometry of the analyzed devices, the numerical model of the process could be implemented in the 2D axis-symmetric space, which radically accelerated the computations and facilitated the presentation and analysis of the results. The calculations of the electromagnetic field were carried out on the universal solver of differential equations based on the FEM method – GetDP software.

Since the alternating electromagnetic field used in the devices featured a quasi-static nature, the calculations were carried out in the symbolic domain with the approach based on the vector magnetic potential. As a result, the determination of the

electromagnetic field distribution came down to solving a single differential equation:

$$\nabla \times \left( \frac{1}{\mu} \nabla \times \mathbf{A} \right) = \mathbf{J}_s + \mathbf{J}_e \quad (1)$$

where:  $\mu$  – magnetic permeability,  $\mathbf{A}$  – magnetic vector potential,  $\mathbf{J}_s$  – source current density,  $\mathbf{J}_e$  – induced eddy currents density.

The eddy currents density was defined by the following equation:

$$\mathbf{J}_e = -\sigma(j\omega \mathbf{A} + \nabla \mathbf{V}) \quad (2)$$

where:  $\sigma$  – electric conductivity,  $\mathbf{V}$  – electric scalar potential.

The distribution of magnetic induction was determined from the distribution of the magnetic vector potential on the basis of the following relationship:

$$\mathbf{B} = \nabla \times \mathbf{A} \quad (3)$$

On the basis of solution of the above equations the Joule heat (4) and the volumetric density of the time-average electromagnetic force (5) were determined:

$$q = \frac{|\mathbf{J}_e|^2}{\sigma} \quad (4)$$

$$\mathbf{f}_L = \frac{1}{2} \text{Re}(\mathbf{J} \times \mathbf{B}^*) \quad (5)$$

where  $\mathbf{B}^*$  is the complex conjugate of  $\mathbf{B}$ .

The mentioned the Lorentz force acts only on the surface layer of liquid metal, the thickness of which depends on the penetration depth of the electromagnetic field:

$$\delta = \sqrt{\frac{2}{\sigma \mu \omega}} \quad (6)$$

where:  $\sigma$  – electrical conductivity of the charge,  $\mu$  – magnetic permeability of the charge,  $\omega$  – angular frequency of the electromagnetic field.

When high frequency fields are used in electromagnetic levitation, for simplicity, it can be assumed that the depth of penetration of this field compared to the size of the charge is 0. This is especially the case for large-scale charges.

The approval of this simplification makes it possible to describe the phenomenon of the action of the Lorentz force on liquid metal with the magnetic pressure (7). The approach facilitates the comparative analysis of the solutions discussed. This pressure pushes the external surface of the liquid metal and is the basic mechanism of metal levitation.

$$p_m = \frac{|\mathbf{B}|^2}{2\mu} \quad (7)$$

where:  $\mathbf{B}$  – magnetic induction,  $\mu$  – magnetic permeability of the charge.

The  $\Delta p$  balance determines whether the outflow of liquid metal placed in the electromagnetic field at the bottom of the levitating charge takes place. The balance consists of: surface tension forces acting towards the convex charge center  $p_s$ , the

above mentioned magnetic pressure  $p_m$  acting in the same direction, and hydrostatic pressure  $p_g$  acting outside the charge.

$$\Delta p = p_g - p_s - p_m \quad (8)$$

If the value of hydrostatic pressure (9) exceeds the total value of the surface tension forces (10) and magnetic pressure (7), the leakage of metal from the charge at the bottom occurs.

$$p_g = \rho gh \quad (9)$$

$$p_s = \gamma \left( \frac{1}{R_1} + \frac{1}{R_2} \right) \quad (10)$$

Where:  $\rho$  – metal density,  $g$  – gravitational acceleration,  $h$  – height of metal column,  $\gamma$  – surface tension,  $R_1$  and  $R_2$  – radii of surface curvature.

A brief analysis of the relations which describe the surface tension forces and hydrostatic pressure reveals the fact that together with the increase of the charge size (height  $h$ , radii  $R_i$ ), the hydrostatic pressure increases as well and the value of the counteracting surface tension pressure decreases. This means that alongside with an increase of the size of charge, the importance of magnetic pressure in the leakage prevention of liquid metal grows.

The model takes into account positioning of the charge, whose actual vertical position  $y$  in the system depends on the balance of two forces acting on the charge i.e. the Lorentz electromagnetic force  $\mathbf{F}_g$  and the force of gravity  $\mathbf{F}_L$ .

$$\mathbf{F}_g(y) - \mathbf{F}_L(y) = 0 \quad (11)$$

where the Lorentz force acting on the entire charge is described by the equation:

$$\mathbf{F}_L = \int_V \mathbf{f}_L dv \quad (12)$$

The force of gravity acting on the entire  $V$ -volume load describes the following relationship:

$$\mathbf{F}_g = V\rho\mathbf{g} \quad (13)$$

### 3. Numerical analysis

Comparative tests were carried out on the example of titanium melting. The metal is characterized by its high degree of reactivity, which makes it very difficult to melt in conventional crucible furnaces. The computations carried out were made for 1 kg charges. For the levitation melting equipment developed so far, such amount of charge was unobtainable which would be demonstrated during the analysis of the classical system.

### 4. Conventional system of levitation melting

In the conventional levitation melting system, the charge is positioned in the axis of the device. A wide variety of modifica-

tions to this system have been developed that use different geometries of the inductor and additional supporting parts. However, all these solutions share the same common disadvantage related to the physics of electromagnetic field – the lack of support of the charge by electromagnetic forces in the axis of the system.

Although the analysis which aimed at explaining this phenomenon was carried out on a relatively simple system consisting only of the inductor, the conclusions derived are representative for any systems in this group. The geometry of the system is shown in Fig. 1. The spiral inductor consists of two parts. The lower bowl-shaped part generates an electromagnetic field that, due to the Lorentz force, causes levitation of the charge. The upper part of the inductor, through which the current flows in the opposite direction than in the lower one, is to stabilize the charge and prevent its escape through the top.

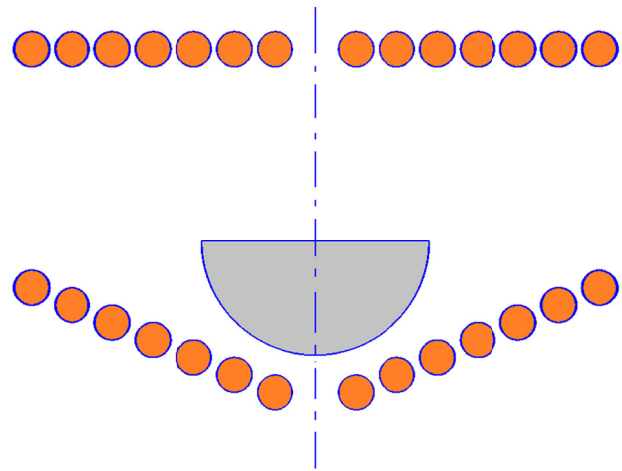


Fig. 1. Conventional levitation melting system with centrally positioned charge

In order to facilitate the analysis, it was assumed that the liquid charge has a constant, simplified hemispherical shape, which approximates the actual shape of the charge in the conventional levitation melting system. The vertical position of the charge resulting from the equation of gravity and the Lorentz force was determined by the iterative method starting from the position in the middle of the system height. The adopted parameters of the model are presented in Table 1.

TABLE 1

Charge properties, geometric data and power parameters of the new system

|                                   |                        |
|-----------------------------------|------------------------|
| Charge radius                     | 0.049 m                |
| Charge weight                     | 1 kg                   |
| External diameter of inductor     | 0.129 m                |
| Distance between 2 inductor parts | 0.087                  |
| Supply current                    | 1000 A                 |
| Supply frequency                  | 10 kHz                 |
| Density of liquid titanium        | 4160 kg/m <sup>3</sup> |
| Conductivity of liquid titanium   | 6·10 <sup>5</sup> S/m  |
| Surface tension of titanium       | 1.7 N/m                |

Fig. 2 shows the distribution of time-averaged Lorentz force lifting the charge and is determined for the inductor current equal 1000 A, approximately the minimum current which assures levitation of the charge. The figure clearly shows the basic problem of the conventional system with the charge positioned in the axis of the device, namely the lack of electromagnetic forces supporting the charge at its critical point – the bottom center.

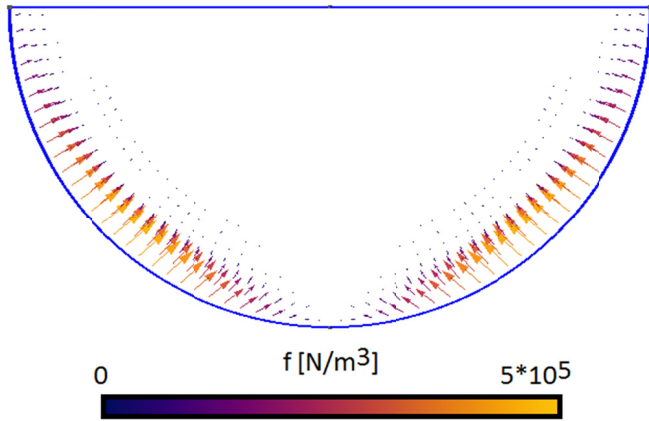


Fig. 2. Distribution of the Lorentz force in the system with centrally positioned charge (1000 A current)

The analysis of magnetic and hydrodynamic pressure distribution on the lower surface of the charge (Fig. 3) indicates that in its large part the magnetic pressure is not able to impede metal leakage due to the hydrostatic pressure. As mentioned in the introduction, in the case of small charges, metal outflow in this area is blocked by surface tension forces. However, in the case of mass and weight of the analyzed titanium charge, the value of the pressure being the result of the surface tension amounts to 70 N/m<sup>2</sup>. As the diagram shows it is negligibly small in comparison with both magnetic and hydrodynamic pressures which are present in the process. Therefore, with such big charges the surface tension does not solve the problem of metal leakage in their axis.

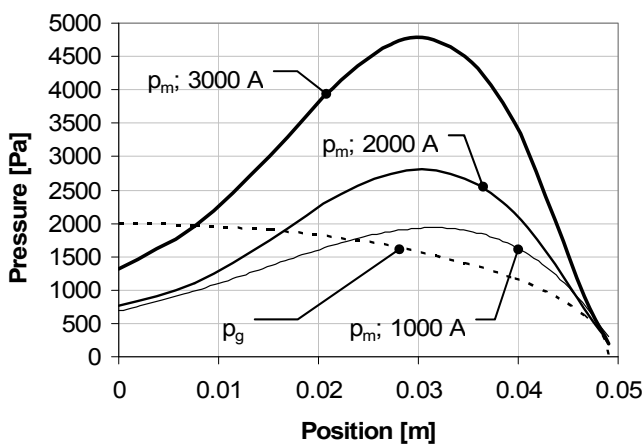


Fig. 3. Distribution of magnetic pressure  $p_m$  and hydrostatic  $p_g$  along the charge radius in conventional system with centrally positioned charge

Raising the current value up to 3000 A in order to increase the value of forces acting on the charge does not solve the prob-

lem. By increasing the power supply of the device to 300 kW which is not easy to be obtained, only a small reduction of the area where magnetic pressure cannot hamper the hydrodynamic pressure was achieved. This confirms the weight of the construction defect of the classical levitation melting device.

## 5. New system of levitation melting

As the previous analysis showed, the limitations of the classical levitation melting system operation, as far as the charge size is concerned, result from the vanishing of electromagnetic field in the axis of the system. The basic idea of the proposed new solution is to remove the charge out of this area. Fig. 4 shows the new levitation melting system. In this system, the charge is a toroid with a semicircular cross-section and is lifted by the electromagnetic field which is generated by the gutter-shaped inductor. In order to make the comparison of both solutions simpler, an inductor with a cross-section similar to that operating in the previous solution was used. It should be remembered though, that the coils of the lower part of the inductors formed a shape of a bowl or a gutter respectively. Table 2 presents geometrical data and power parameters of the inductor. For the sake of simplicity, a static half-toroidal shape of a charge was assumed for the computations. Its position in the system was determined on the basis of the balance of gravity and the Lorentz force.

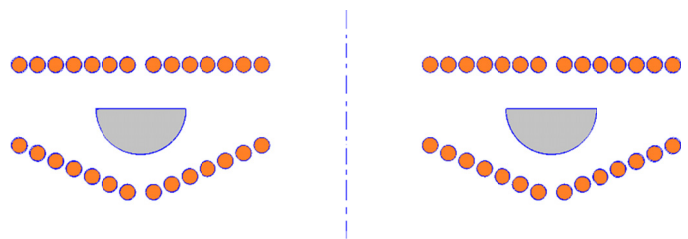


Fig. 4. Cross-section through the axis of symmetry of the new levitation melting system

Fig. 5 presents the distribution of the Lorentz force density field for the proposed system. A brief analysis proves that the main problem of the conventional system does not appear here.

TABLE 2

Geometric data and power parameters of the new system

|  |          |
|--|----------|
| Radius of the charge ring                | 0.080 m  |
| Charge cross-section radius              | 0.0175 m |
| Weight of the charge                     | 1 kg     |
| Internal diameter of the inductor        | 0.030 m  |
| External diameter of the inductor        | 0.129 m  |
| Distance between 2 parts of the inductor | 0.025    |
| Supply current                           | 300 A    |
| Supply frequency                         | 40 kHz   |

Due to the charge removal out of the device axis, its entire bottom surface was supported by electromagnetic forces. The

forces acting on the charge from the top (see the Figure) were the result of an impact the electromagnetic field, which is generated by the upper stabilizing part of the inductor, exerted upon the charge. The effect was revealed due to the more central vertical position of the charge in the device under analysis (Fig. 4) than in the device previously described (Fig. 1).

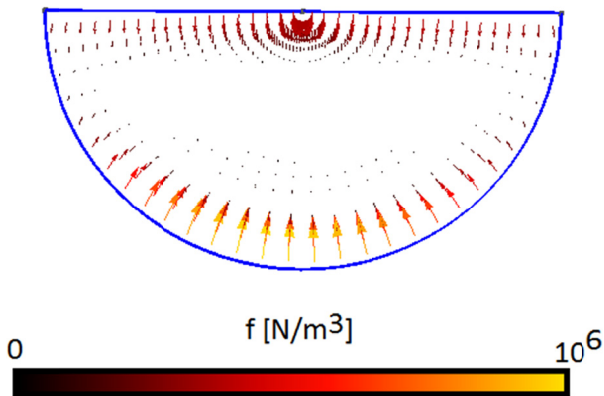


Fig. 5. Distribution of the Lorentz force density acting on the charge (current 300 A)

Analysis of the pressure distribution acting on the lower surface of the charge (Fig. 4) indicates that the magnetic pressure is much higher than the hydrostatic pressure over the entire charge width. It becomes clearly visible in the most sensitive bottom point of the load. The lack of symmetry in the distribution of magnetic pressure, despite the symmetry of the cross-section of the charge and the inductor, results from the decrease of electromagnetic forces as they approach the axis of the system.

The main purpose of the levitation melting process is to heat up and maintain the charge temperature. The charge is heated both by the eddy currents induced through the electromagnetic field in the charge and generation of Joule heat. Fig. 5 presents the distribution of the heat density field generated in the charge in the proposed levitation melting device. The total power generated in the charge is 34 kW, with a power consumption of 60.7 kW. This means that the electrical efficiency of the

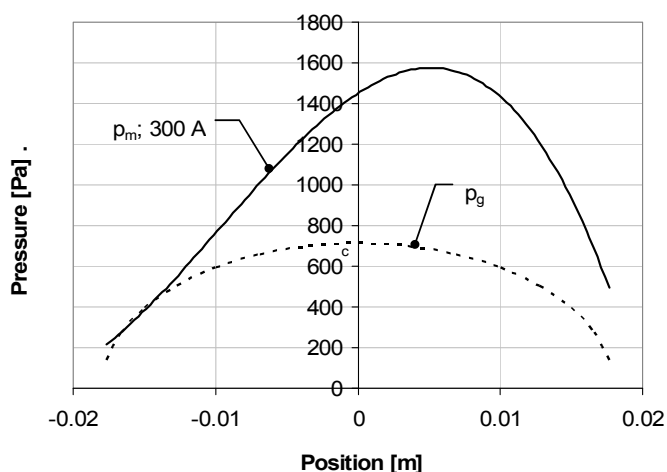


Fig. 6. Distribution of hydrostatic pressure  $p_g$  and magnetic  $p_m$  at the bottom of the charge

analyzed device is 56%, which is a much higher value than that found for the cold crucible device [2]. Additionally, unlike in the case of semi-levitation cold crucible device, there is no heat escape through the bottom of the crucible. Therefore, the overall efficiency of the analyzed device is much higher than the one with a cold crucible.

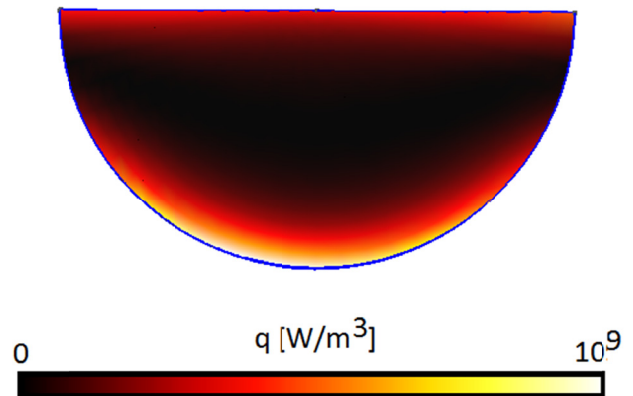


Fig. 7. Distribution of the Joule heat density field generated in the charge

## 6. Discussion and summary

The carried out analysis showed that the conventional levitation melting system contains, due to the physics of the electromagnetic field, a defect which cannot be corrected easily. It is the vanishing field in the charge axis. When the hydrostatic pressure related to the mass of the molten charge can no longer be compensated by the surface tension forces, the liquid metal escapes from the device.

The newly developed levitation melting system proposed in the article is not burdened with this defect. Numerical analysis confirmed that the system is able to melt charges as heavy as 1 kg, which previously was not possible to be performed with the application of the existing devices. Besides, a radical change in the design of the device allows scaling for virtually any amount of charge. The only restrictions here is the availability of power sources which can provide a suitable high current. As an additional advantage of the proposed solution, the use of a single-frequency field, which greatly facilitates the development of appropriate power sources for the device should be mentioned.

Due to its high efficiency, the device can be an interesting alternative to the cold-water semi-levitation devices used for melting reactive metals.

The numerical analysis confirmed the validity of the concept of a new levitation melting device and may be the basis for undertaking the financial risk of constructing a prototype for large-scale levitation melting.

## Acknowledgements

This paper has been financially supported by Ministry of Science and Higher Education within the framework of the BK-221/RM0/2018.

## REFERENCES

- [1] P. Buliński, J. Smolka, S. Golak, R. Przyłucki, M. Palacz, G. Siwiec, ... & L. Blacha, *International Journal of Heat and Mass Transfer* **126**, 980-992 (2018).
- [2] S. Golak, R. Przyłucki, J. Smolka J.P. Bulinski, P. Cieplinski, *International Journal of Applied Electromagnetics and Mechanics* **56** (2), 165-172 (2018).
- [3] V. Nemkov, R.C. Goldstein, K. Kreter, J. Jackowski, *Proceedings of the International Conference on Heating by Electromagnetic Sources, HES-13*, (2013).
- [4] G. Sugilal, S. Kumar, M.H. Rao, S.K. Mishra, J. Jha, K. Banerjee, G.K. Dey, *Development of induction skull melting technology, BARC Newsletter* **348**, 50-55 (2015).
- [5] O. Muck. *German Patent 422004* (1923).
- [6] S. Spitans, E. Baake, B. Nacke, A. Jakovics, *Magnetohydrodynamics* **51** (1), 121-132, (2015).
- [7] T. Merder, J. Pieprzyca, *Metalurgija* **50** (4), 223-226 (2011).
- [8] M. Warzecha, T. Merder, P. Warzecha, G. Stradomski, *ISIJ International* **53** (11), 1983-1992 (2013).
- [9] X.K. Lan, J.M. Khodadadi, *International Journal of Heat and Mass Transfer* **44** (5), 953-965 (2001).
- [10] R. Bölling, H.J. Odenthal, H. Pfeifer, *Steel Research International* **76** (1), 71-80 (2005).
- [11] M.J. Cho, C. Kim, *The Iron and steel Institute of Japan International* **46** (10), 1416-1420 (2006).
- [12] T. Jormalainen, S. Louhenkilpi, *Steel Research International* **77** (7), 472-484 (2006).
- [13] C Bruch, P. Valentin, *Steel Research International* **75** (10), 695-665 (2004).
- [14] S.K. Mishra, P.K. Jha, S.C. Sharma, S.K. Ajamani, *Canadian Metallurgical Quarterly* **51** (2), 170-183 (2012).
- [15] A. Fornalczyk, S. Golak, R. Przyłucki, *Archives of Civil and Mechanical Engineering* **15** (1), 171-178 (2015).
- [16] A. Fornalczyk, S. Golak, M. Saturnus: *Mathematical Problems in Engineering*, 461085, 2013.
- [17] M. Saturnus, T. Merder, P. Warzecha, *Numerical modelling of the hydrogen removal process from liquid aluminium, International Conference Liquid Metal Processing and Casting*, Edited by M. Krane, R. Williamson, J.P. Bellot and A. Jardy, SF2M, 329-336 (2011).
- [18] E. Ramos-Gomez, R. Zenit, C. Gonzalez-Rivera, G. Trapaga, M. Ramirez-Argaez, *Metall. Mater. Trans. B* **44**, 423-435 (2013).
- [19] V.S. Warke S. Shankar, M.M. Makhlof, *Journal of Materials Processing Technology* **168**, 119-126 (2005).
- [20] V.S. Warke, G. Tryggvason M.M. Makhlof, *Journal of Materials Processing Technology*, **168**, 112-118 (2005).
- [21] B. Wana, W. Chena, M. Mao, Z. Fu, D. Zhu, *Journal of Materials Processing Tech.* **251**, 330-342 (2018).